A benchmarking study for CINEMA and MELCOR codes subject to core degradation phase of PHÉBUS FPT 1 by using dynamic time warping

Joon Young Bae [a], Chang Hyun Song [a], Wonjun Choi [a], Dong Gun Son [b], Jun Ho Bae [b], Sung Joong Kim [a, c*]
[a]*Department of Nuclear Engineering Hanyang Univ., 222, Wangsimni-ro, Seongdong-gu Seoul, Korea*
[b]*Korea Atomic Energy Research Institute, 1045, Daedeok-daero, Yuseong-gu, Daejeon, Korea*
[c]*Institute of Nano Science and Technology, Hanyang Univ., 222 Wangsimni-ro, Seongdong-gu, Seoul, Korea*
[*]*Corresponding author: sungjkim@hanyang.ac.kr*

1. Introduction

The integrated severe accident (SA) analysis codes support accurate calculation of various SA phenomena and prediction of resulting source terms. The performance of the SA codes can be improved by validating against separate or integrated effect experiments, and measured data from actual accident in nuclear power plant (NPP) such as TMI-2 accident [1].

Code for INtegrated severe accident Evaluation and MAnagement (CINEMA) is a newly integrated SA analysis code being developed in Republic of Korea. As shown in Figure 1, CINEMA is structured with multiple modules such as CSPACE (In-vessel phenomena analysis module), SACAP (Ex-vessel phenomena analysis module), and SIRIUS (Fission product behavior analysis module). The MASTER platform supports the physical linkage between individual modules mentioned above. As a stand-alone SA code, CINEMA can analyze the entire process of SAs from the core heat-up to the containment rupture of light water reactor [2].

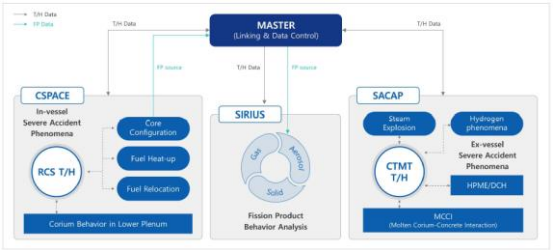

Fig. 1. Structure of CINEMA [2]

Being as a part of CINEMA User Group activities to improve the prediction capability, the objective of this paper is to validate models in CINEMA code by benchmarking reliable experimental data. Among diverse and complex phenomena entailed in SA, core degradation was selected as imminent target phenomenon because it plays an initial condition for both in/ex-vessel phenomena in NPP [3]. In other words, the credibility of subsequent phenomena simulations can be increased if the core degradation can be predicted accurately.

In this paper, a core degradation model in CINEMA code was assessed by benchmarking PHÉBUS FPT 1 experiment. MELCOR simulation for the same experiment was also conducted for comparative purpose. As a result, some of actual experimental data, MELCOR calculation results, and CINEMA calculation results were analyzed. Then, results are compared by using Dynamic Time Warping (DTW) method to evaluate similarity of trends of different time-series.

2. Methodology

In this section, target experiment of benchmark is summarized. Also, methods adopted for benchmarking (using CINEMA 2.0 and MELCOR 2.1.6840) are introduced.

2.1 Benchmark target experiment: PHÉBUS FPT 1

The purpose of PHÉBUS Fission Product (FP) program is to understand the core degradation and behavior of fission products under SAs. PHÉBUS FP test facility was designed to be scaled down by a factor 5,000 in volume relative to a 900 MWe Light Water Reactor [4]. A schematic of PHÉBUS FP test facility is shown in Figure 2; a reactor core and test section, hot leg, steam generator U-tube, cold leg, and containment with sump. As steam passes through the test section, it heats up fuel rods and flows to the hot leg. Then, steam, including FPs, is cooled in a steam generator, and collected in a containment via a cold leg. It should be noted that the scope of this paper is limited to the core degradation phase in this experiment, not FP behaviors.

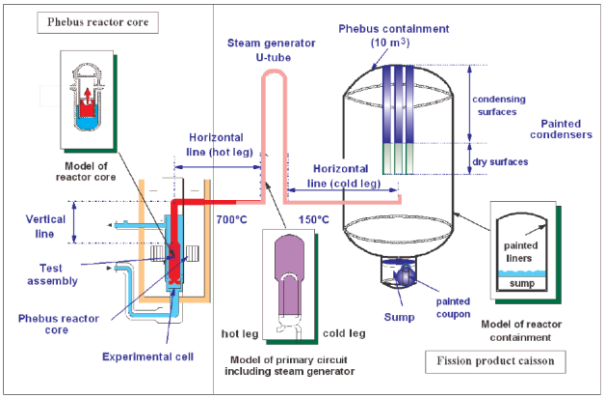

Fig. 2. A schematic of PHÉBUS-FP experimental facility [5]

The PHÉBUS FPT series consist of 5 tests from FPT 0 to FPT 4. In this paper, FPT 1 was used as the benchmarking target. The main features of FPT 1 are summarized in Table 1. FPT 1 experiment was implemented with an Ag-In-Cd control rod as a

representative of Westinghouse-type Pressurized Water Reactors [4].

Table 1: Major features of FPT 1 [6]

Fuel Condition	Control Rod (wt %)	Purpose
23 GWD/MTU Burn-up rod (20 EA)	Ag-In-Cd 80:15:5 (1 EA)	Core Damage & Max FP release under steam rich condition

Figure 3 shows steam flow rate and power history of FPT1 experiment. The steam flow rate injected into the test section varied from 1.0E-6 kg/s to 2.21E-3 kg/s. Thermal power varied from 0 kW to 43 kW, which is the sum of the fission and decay power.

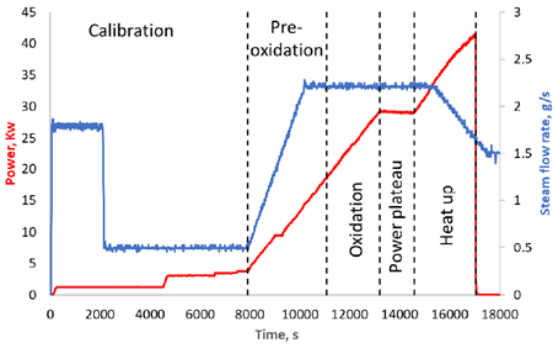

Fig. 3. Steam flow rate & power, experimental [7]

2.2 Numerical calculation methods

Input decks of CINEMA and MELCOR for PHÉBUS FPT 1 were developed [2, 8]. Each input is based on PHÉBUS FPT 3 CINEMA and MELCOR input by emending steam flow rate, control rod configuration, power, shroud configuration, steam temperature, etc. [9]. Being unable to approach some fundamental documents like FPT 1 final report, data book or specification on ISP-46, nodalizations and geometries still have room for improvement for FP behavior and oxidation heat properties in CINEMA input. Figure 4, 5, and 6 show PHÉBUS system nodalization, core nodalization, and shroud – pressure tube configuration, respectively.

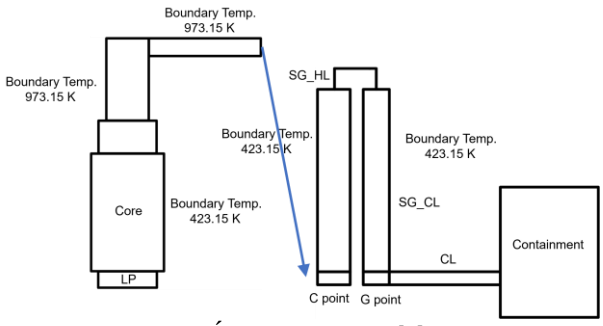

Fig. 4. PHÉBUS system nodalization

In figure 4., nodalization consisted of 24-severe accident module, 7-hydraulic cell, and 6-heat structure. To prevent system heat loss, 973.15 K was set as the boundary temperature condition at the riser and the hot leg, and 423.15 K was set as the boundary condition for the cold leg and the steam generator for cooling.

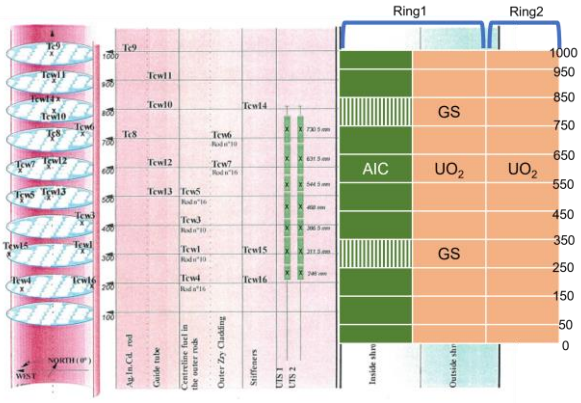

Fig. 5. Core nodalization

In Figure 5., 1 m active core region was composed of 11 axial levels and 2 radial rings. An Ag-In-Cd control rod only existed in ring 1.

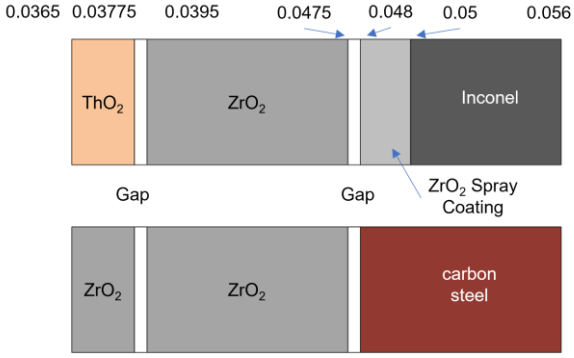

Fig. 6. Shroud – Pressure Tube Configuration

As seen in Figure 6., the shroud surrounding the fuel was not properly implemented in CINEMA. In the actual experiment of (a), the thoria layer and the zirconia layer of the shroud was separated up and down. In CINEMA of (b), however, it is impossible to separate layers. So only the zirconia layer was used for simulation. Also, materials and reactor components in CINEMA are hard-wired to each other, there is little flexibility in input. That is the reason that the configuration like (b) came out. To solve this problem, as a temporary measure, the heat loss was adjusted by appropriately tuning the heat transfer coefficient.

The initial conditions for simulation such as inlet steam flow rate, steam temperature, and pressure, to mention a few are the same for both MELCOR and CINEMA. Two of the conditions commonly applied to MELCOR and CINEMA are indicated in Figure 7.

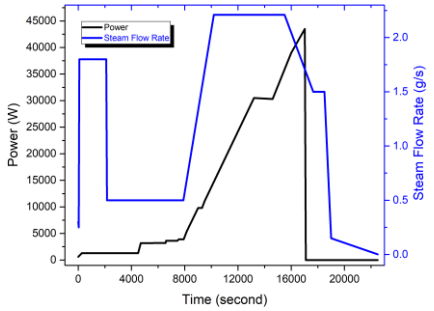

Fig. 7. Total power and steam flow rate applied to both MELCOR and CINEMA

2.3 Similarity Measurement: Dynamic Time Warping

In this paper, Dynamic Time Warping (DTW) method, which is actively utilized in various fields, was used for quantitative assessment of MELCOR and CINEMA benchmarking results. As will be shown in Section 3, although the progression patterns of the two time-series are similar with each other, if the timing of the progression is different, it is difficult to confirm the similarity with Euclidean Distance (ED) because Euclidean distance only compares distances from the same time step. DTW is one of algorithms that determines the similarity, not consistency between two time-series data that have different lengths each other. Figure 8 shows the difference between ED and DTW.

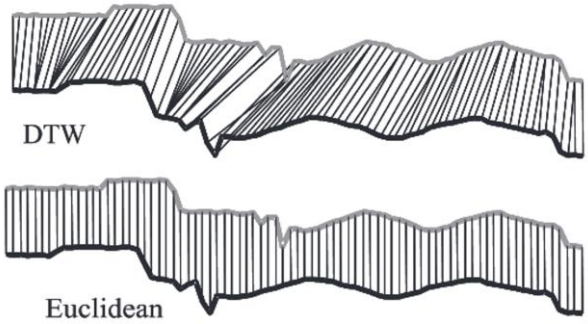

Fig. 8. DTW distance and Euclidean distance [10]

In Figure 8, the gray time-series and the black time-series share the same type, but the gray time-series includes a time delay compared to the black time-series. ED does not reflect such time delay, speed difference, etc., because it is sensitive to distortion on the time axis. On the other hand, DTW can catch a similar pattern. Because similarity is the inverse of distance, as the distance between the two time-series is short, it means that the similarity between the time series can be confirmed. By using DTW, similarity can be defined quantitatively, compared to ED, which has a relatively large error with respect to time axis distortion. Particularly, even if the points of a specific peaks are different and the shapes are similar, the distance is shortened. Therefore, the feature of DTW is such that trend comparison makes possible.

While DTW certainly has advantages over conventional ED in measuring the similarity of trends, DTW also exhibits weaknesses: where a relatively small section of one sequence maps onto a relatively large section of another [10]. This leads to underestimation of the distance between time-series. Therefore, Sakoe-Chiba band as a global constraint with ~5 % of length of time-series of warp window size was used in this analysis [11]. In other words, when the time axis between the two time-series differs by more than 5%, there is a limit to prevent further mapping. In this case, if the shape of the peak as well as the time point of the peak are more than 5% away from the time axis, the distance increases, and the similarity decreases. Therefore, the difference between the time and the shape can be considered at the same time, in contrast to the unconstrained DTW, where only shapes can be compared.

3. Result and Discussion

3.1 Analysis of CINEMA and MELCOR simulation results

As part of Software Quality Assurance, validation should avoid trying to tune results [12]. Therefore, the results presented in this paper did not go through the process of tuning the calculation results to the reference data after the sensitivity analysis. The results of MELCOR and CINEMA were different from each other by simulating the experiment without changing the default value of the oxidation model in each code.

Since actual FPT 1 data were inaccessible, reference data were extracted from P. Darnowski et al. by using WebPlotDigitizer, an open-source, semi-automatic digitizer [13, 14]. Between results of CINEMA and MELCOR calculations, fuel temperature, cladding temperature, core outlet steam temperature, the rate and amount of hydrogen generation were compared among three datasets.

Figures 9 and 10 are fuel temperatures at 300 and 400 mm from the bottom of fuel bundle. At green circle in Figure 9, MELCOR predicts the temperature behavior relatively well with respect to experimental values, whereas CINEMA does not. MELCOR also predicts few temperature peaks due to oxidation heat in the orange circle of Figure 10. On the other hand, CINEMA result did not show any temperature peak.

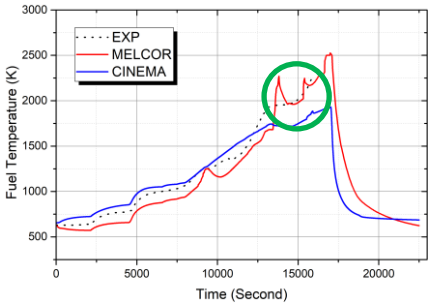

Fig. 9. Fuel temperature at 300 mm from the bottom of fuel bundle

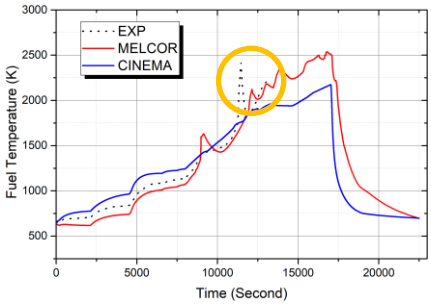

Fig. 10. Fuel temperature at 400 mm from the bottom of fuel bundle

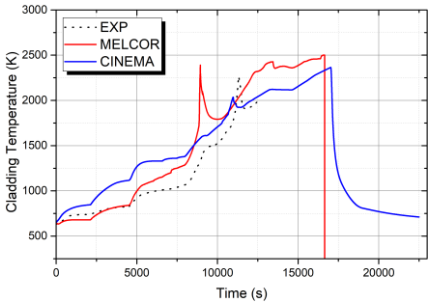

Fig. 11. Clad temperature at 600 mm from the bottom of fuel bundle

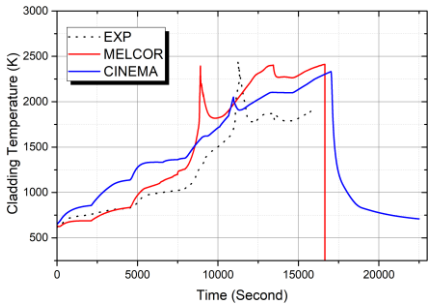

Fig. 12. Clad temperature at 700 mm from the bottom of fuel bundle

Figures 11 and 12 show the cladding temperature at 600 and 700 mm, respectively. The cladding in MELCOR simulation was melted and relocated at about 16,545 seconds, whereas that of CINEMA was not melted as the melting point was not reached. As mentioned in Section 2.2, it is presumed that this is the consequence of not properly reflecting the oxidation heat generated.

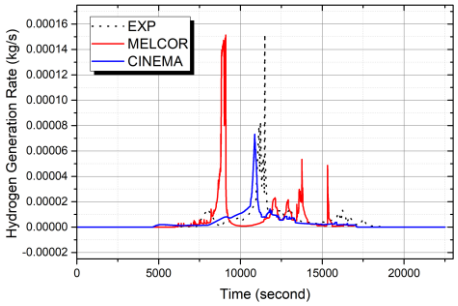

Fig. 13. Total hydrogen generation rate

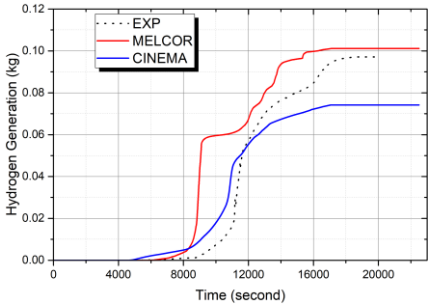

Fig. 14. Total hydrogen generation

Oxidation results as well as core degradation were analyzed. Figures 13 and 14 show that total generation rate of hydrogen and accumulated hydrogen mass, respectively. The peak of the hydrogen generation rate was observed in MELCOR (1.45558E-4 kg/s at 9,095 second) was agreed better with the reference data (1.49921E-5 kg/s at 13,092 second) than that of CINEMA (7.10887E-5 kg/s at 10,865 second). However, the timing at the highest peak was more accurate with CINEMA. Meanwhile, accumulated hydrogen mass predicted by MELCOR was closer to the reference data than that of CINEMA.

MELCOR calculation results were similar to the experimental hydrogen generation rates, although the timing of the peak hydrogen generation rate was better predicted by CINEMA. It is presumed that the simulation of the experiment without changing the default value of the oxidation model in each code led to the result of less oxidation in CINEMA.

Overall, oxidation occurred faster and more frequently in MELCOR than in CINEMA, which is presumed to be due to the difference in the debris formation model. In CINEMA, when the cladding reaches a certain temperature (1173 K), it begins to shatter, and when it becomes a debris layer, oxidation does not occur. In contrast, in MELCOR, debris formation model was not set, resulting in more oxidation.

3.2 Comparison using Dynamic Time Warping

Since the reference data could not be extrapolated (All reference data used in this paper were obtained truncated before 20,000 seconds), the computational results for MELCOR and CINEMA were analyzed after being truncated to fit the reference data length. Also, for

comparison between parameters with different orders, the parameters were normalized through min-max scaling.

Table 2 shows the DTW and ED values for each item analyzed in Section 3.1.

Table 2. DTW vs. ED Distance

	DTW Distance		ED	
Comparison w/ Ref.	MELCOR vs. Reference	CINEMA vs. Reference	MELCOR vs. Reference	CINEMA vs. Reference
Fuel temperature at 300 mm	2.63877	6.14371	8.65723	10.07454
Fuel temperature at 400 mm	2.87675	4.27089	7.34415	8.06340
Clad temperature at 600 mm	5.97116	6.94466	13.57251	15.21631
Clad temperature at 700 mm	16.67174	11.49629	21.76564	18.88296
H2 generation rate	14.20107	3.02338	17.86648	9.11498
Accumulated H2 generation	7.41674	13.51013	26.16939	16.16242

In Table 2, after making the time steps of each time-series the same through linear interpolation, the ED distance was obtained.

Since the inverse of the distance represents similarity, the smaller the value in the table above, the more similar to the reference data. Also, DTW is lower than ED because DTW represents the optimized distance. Overall, it is observed that MELCOR simulated the actual experiment better than CINEMA. In accumulated H2 generation, however, the order of magnitude of MELCOR and CINEMA values was reversed in DTW, and ED. Figure 12 shows the optimal path for two time series using DTW and ED.

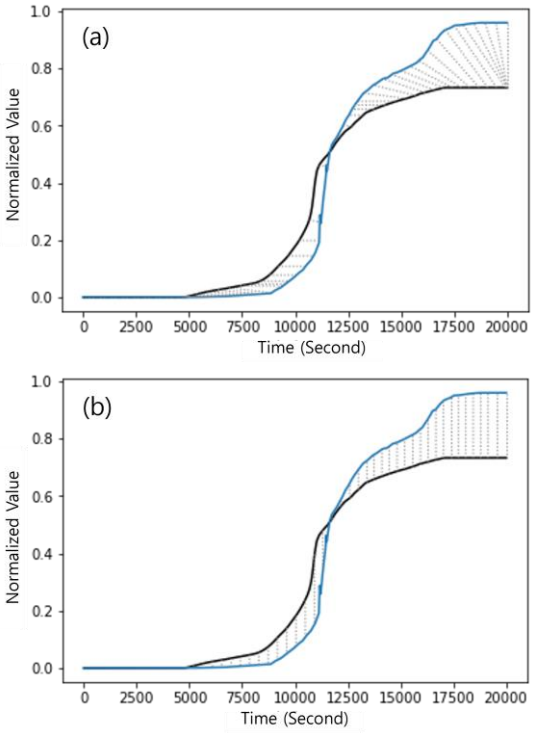

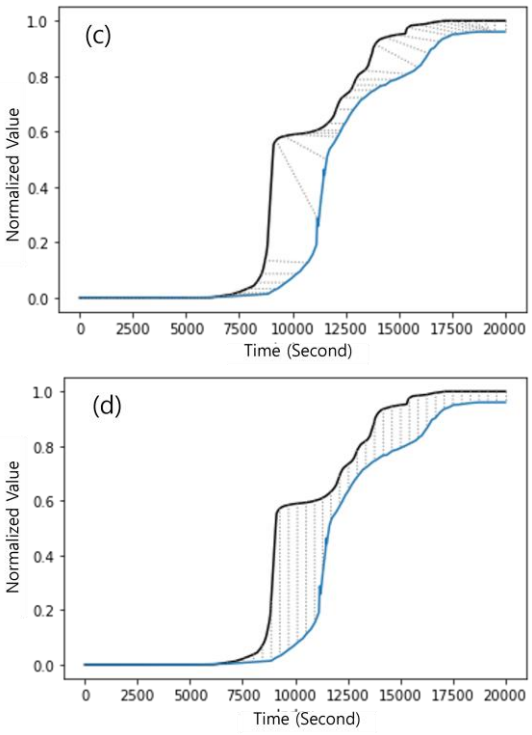

Fig. 15. (a), (b) DTW distance and ED distance in normalized, accumulated hydrogen generation mass between CINEMA (black line) and Reference data (blue line)
(c), (d) DTW distance and ED distance in normalized, accumulated hydrogen generation mass between MELCOR (black line) and reference data (blue line)

As seen in Figure 14, generation quantity of experimental data is much similar to those of MELCOR than those of CINEMA. However, ED between MELCOR/CINEMA calculation results and reference data did not imply such result. Rather, in ED, the CINEMA calculation result appears closer to the experimental result in Table 2. When comparing (b) and (d) in Figure 15, euclidean distances of CINEMA vs. Reference and MELCOR vs. Refence, in (a), there is a relatively slight difference in vertical distance in the second half, whereas in (d) there is a relatively large difference in overall vertical distance.

As DTW is invariant to time shifts between series, Horizontal distances within the 2000 second range are counted as zero in DTW (The 2000 second limit is due to the Sakoe-Chiba band). The CINEMA result in (a) has some vertical distance from the reference time series, whereas the MELCOR result in (c) is similar to the left offset of the reference time series, so the DTW distance in (c) is smaller. This is why the DTWD and ED results of the accumulated H2 generation items in Table 2 are opposite to each other.

4. Conclusions

In this paper, numerical simulations of PHÉBUS FPT 1 were preliminarily conducted by using both CINEMA and MELCOR and their results were compared to reference data to validate the core degradation model of CINEMA. In addition, the similarity between the reference data and the calculated data was quantitatively evaluated by using DTW. As a result of comparison, MELCOR calculation results were more similar to experimental values at FUEL temperature, cladding temperature at 600 mm, and accumulated hydrogen, and CINEMA calculation results showed similar trends to experimental values at cladding temperature at 700 mm and hydrogen generation rate. It is judged that the oxidation model used in MELCOR simulated the experiment better. In a future work, as more data are collected, the CINEMA nodalization of PHÉBUS FPT1 will be accurately defined with modifying default values of oxidation model in CINEMA, and input of FP behavior will also be included in CINEMA input deck.

ACKNOWLEDGEMENTS

This work was supported by the Korea Institute of Energy Technology Evaluation and Planning (KETEP) and the Ministry of Trade, Industry & Energy (MOTIE) of the Republic of Korea (No. 20193110100050).

Additionally, this work was supported by the Nuclear Safety Research Program through the Korea Foundation of Nuclear Safety (KoFONS) using the financial resource granted by the Nuclear Safety and Security Commission (NSSC) of the Republic of Korea (grant number 2003006-0120-CG100).

REFERENCES

[1] INTERNATIONAL ATOMIC ENERGY AGENCY, Status and Evaluation of Severe Accident Simulation Codes for Water Cooled Reactors, IAEA-TECDOC-1872, IAEA, Vienna, 2019.

[2] Korea Hydro & Nuclear Power Co., Ltd., User Manual for CINEMA 2.0, 2022.

[3] P Hofmann, Current knowledge on core degradation phenomena, a review, Journal of Nuclear Materials, Volume 270, Issues 1–2, 1999, Pages 194-211, ISSN 0022-3115, https://doi.org/10.1016/S0022-3115(98)00899-X.

[4] Parisot, Jean-François. Research Nuclear Reactors. Paris: Éditions le Moniteur [for] Commissariat à l'énergie atomique et aux énergies alternatives, 2012.

[5] F. Payot, et al., 2011. FPT3 Final Report, IRSN Document Phébus PF IP/11/589, DPAM/DIR-2011.

[6] C. Bratfisch and M. K. Koch, Preliminary results of a comparative as-sessment of ATHLET-CD and MELCOR by simulating the experiment PHEBUS FPT1, in NURETH-16 Conference, 2015, pp. 2143-2156.

[7] N. Elsalamouny and T. Kaliatka, Uncertainty Quantification of the PHEBUS FPT-1 Test Modelling Results, Energies, vol. 14, no. 21, p. 7320, 2021. [Online]. Available: https://www.mdpi.com/1996-1073/14/21/7320.

[8] MELCOR Computer Code Manuals, Vol. 1: Primer and Users' Guide, Version 2.1.6840, SAND 2015-6691 R, Sandia National Laboratories, 2015.

[9] J. H. Bae et al., Core degradation simulation of the PHEBUS FPT3 experiment using COMPASS code, Nuclear Engineering and Design, vol. 320, pp. 258-268, 2017/08/15/ 2017, doi: https://doi.org/10.1016/j.nucengdes.2017.05.030.

[10] E. Keogh and C. A. Ratanamahatana, Exact indexing of dynamic time warping, Knowledge and Information Systems, vol. 7, no. 3, pp. 358-386, 2005/03/01 2005, doi: 10.1007/s10115-004-0154-9.

[11] H. Sakoe, and S. Chiba, Dynamic programming algorithm optimization for spoken word recognition. IEEE Transactions on Acoustics, Speech, and Signal Processing, volume ASSP-26, pp. 43-49, 1978.

[12] L. L. Humphries, MELCOR Code Development Status, presented at the Conference: Proposed for presentation at the European MELCOR User Group held May 2-3, 2013 in Stockholm, Sweden., United States, 2013.

[13] P. Darnowski, M. Włostowski, M. Stępień, and G. Niewinski, Study of the material release during PHÉBUS FPT-1 bundle phase with MELCOR 2.2., 2020.

[14] A. Rohatgi, WebPlotDigitizer: Version 4.5, https://automeris.io/WebPlotDigitizer, 2021.